

Compact all-optical differential-equation solver based on silicon microring resonator

Liyang LU, Jiayang WU, Tao WANG, Yikai SU (✉)

State Key Laboratory of Advanced Optical Communication Systems and Networks, Department of Electronic Engineering, Shanghai Jiao Tong University, Shanghai 200240, China

© Higher Education Press and Springer-Verlag Berlin Heidelberg 2012

Abstract We propose and numerically demonstrate an ultrafast real-time ordinary differential equation (ODE) computing unit in optical field based on a silicon microring resonator, operating in the critical coupling region as an optical temporal differentiator. As basic building blocks of a signal processing system, a subtractor and a splitter are included in the proposed structure. This scheme is featured with high speed, compact size and integration on a silicon-on-insulator (SOI) wafer. The size of this computing unit is only $35\ \mu\text{m} \times 45\ \mu\text{m}$. In this paper, the performance of the proposed structure is theoretically studied and analyzed by numerical simulations.

Keywords ordinary differential equation (ODE), silicon microring resonator, analog signal processing (ASP), silicon-on-insulator (SOI)

1 Introduction

After years of improvement and miniaturization, the integration of electronic devices for information processing is rapidly approaching its fundamental speed and bandwidth limitations. All-optical signal computing technology is a promising solution to overcome the speed limit of the electronic devices. In recent years, several equivalent devices in photonics to those in electronics have been proposed, such as all-optical temporal differentiator [1–3] and all-optical temporal integrator [4]. With the help of these basic building blocks, more complicated optical signal processing devices can be realized.

Several schemes have been proposed for performing real-time signal processing in optical domain. Some are based on finite-impulse-response (FIR) optical digital filters [5], an asymmetric two-arm interferometer for

instance. This method exhibits relatively large physical lengths of the devices [6]. It was also proposed to use fiber-grating devices as analog all-optical processors, such as long-period fiber grating [2] and fiber Bragg grating [7]. These devices can be used to process ultrafast signals, but the device sizes are on the order of several millimeters. Also, some schemes of all-optical analog-to-digital converter (ADC) were proposed to help realizing the analog optical signal processing [8,9], but the limited converting speed is critical for enhancing the performance, and the systems are too complicated to be integrated. To the best of our knowledge, no scheme of on-chip analog all-optical signal processing device, such as an ordinary differential equation (ODE) solver, has been proposed with the features of compact size, high speed and ease of integration.

Differential equations play a central role in the field of signal processing [10]. In virtually any field of science and technology [11], e.g., physics, biology, chemistry, economics and engineering, in-depth study in these equations is always required. All constant coefficient linear differential equations can be modeled as systems with finite number of differentiators, subtractors, splitters and feedback branches [10]. An optical computing device based on this system modeling theory can be easily modified to meet different requirements of different ODEs, and can be concatenated to solve higher-order differential equations. An optical ODE solving unit that features high speed and compact footprint can find its applications in many areas, such as optical processing of radio frequency (RF) signals in radio-over-fiber (RoF) systems [7], pulse shaping [12], and ultra-fast signal processing in optical sensing systems.

In this paper, we propose an ultrafast optical temporal ODE computing unit based on a silicon microring resonator with a radius of $10\ \mu\text{m}$, and investigate the performance of the proposed structure. Several signals with typical waveforms are used in simulation to test the optical ODE solver.

2 Operating principle

An all-optical temporal ODE computing unit is constructed on the basis of a specially designed system block diagram. This unit provides an optical output with one complex envelop that can be interrelated to the other envelop of input optical signal with a specific differential equation. According to the fundamental theory of signals and systems, a linear time-invariant analog signal processing (ASP) system could be realized with a proper combination of basic building blocks, such as differentiators, subtractors and splitters [10]. The block diagram of the first-order differential equation of our design (Eq. (1)) is shown in Fig. 1(a), where a differentiator, a subtractor and a splitter are included. Also a forward path and a feedback branch, as typical elements in a classic frame of signal processing system, are introduced in the diagram. Figure 1(b) shows the complete structure we designed.

$$y + \frac{1}{2} \frac{dy}{dt} = \frac{1}{2} \frac{dx}{dt}. \quad (1)$$

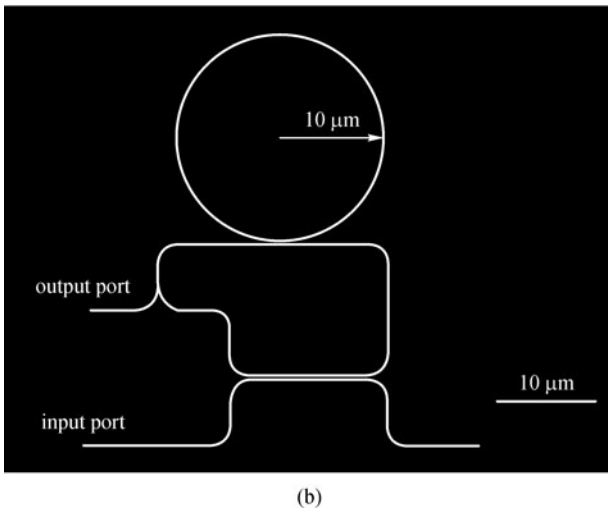
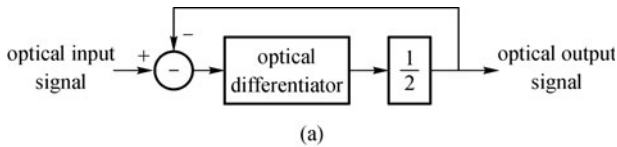


Fig. 1 (a) Block diagram of ODE solving unit; (b) complete structure of optical ODE solver

The subtractor is realized using a 3 dB directional coupler together with an accurate design of the loop length, composing of a forward path and a feedback branch. Figure 2(a) shows the structure of the 3 dB directional coupler, with a slot width of the coupling region of about $0.1 \mu\text{m}$. Equation (2) describes its input-output relation. To achieve 3 dB coupling feature, the coupling length of the

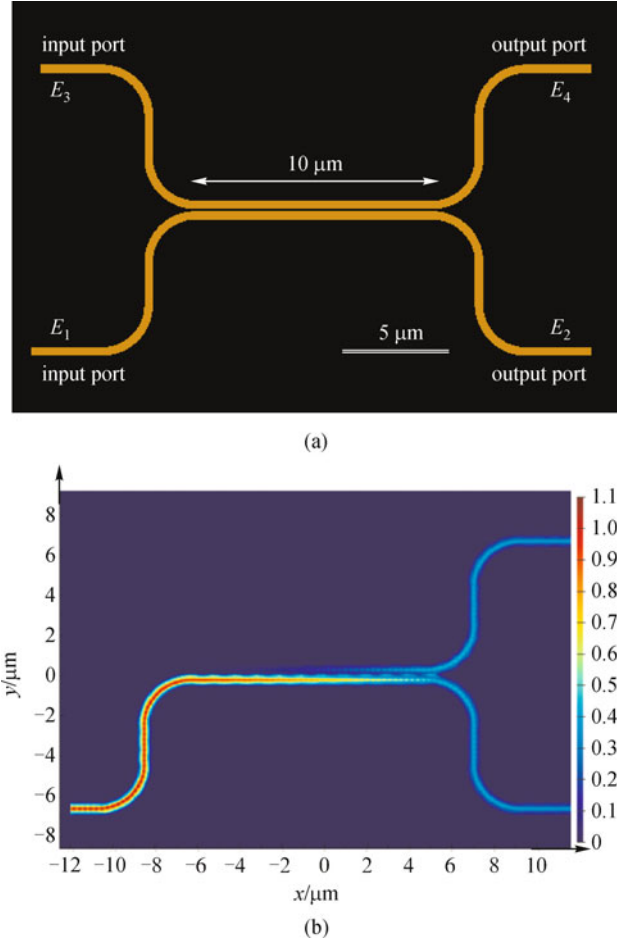


Fig. 2 (a) 3 dB directional coupler; (b) distribution of electric field intensity with an input signal at port 1

directional coupler is about $10 \mu\text{m}$. Figure 2(b) shows the distribution of electric field intensity with an input signal at port 1.

$$\begin{bmatrix} E_4 \\ E_2 \end{bmatrix} = \frac{1}{\sqrt{2}} \begin{bmatrix} 1 & i \\ i & 1 \end{bmatrix} \begin{bmatrix} E_3 \\ E_1 \end{bmatrix}. \quad (2)$$

The design of the whole loop with a 3 dB directional coupler is shown in Fig. 3(a). If we precisely control the loop length to meet the condition that there is a phase shift of $(2n+1)\pi$ along the loop, the relation between E_3 and E_4 will be

$$E_3 = e^{-j(2n+1)\pi} E_4 = -E_4. \quad (3)$$

Equivalent block diagram of the loop can be derived from Eqs. (2) and (3), as shown in Fig. 3(b). There is an additional block with a factor i existing before the loop, which will cause a $\pi/2$ phase shift. However, this will not affect the performance of the structure, since it is outside the loop and can be compensated by the phase shift in the waveguides of input port and output port. The block has a

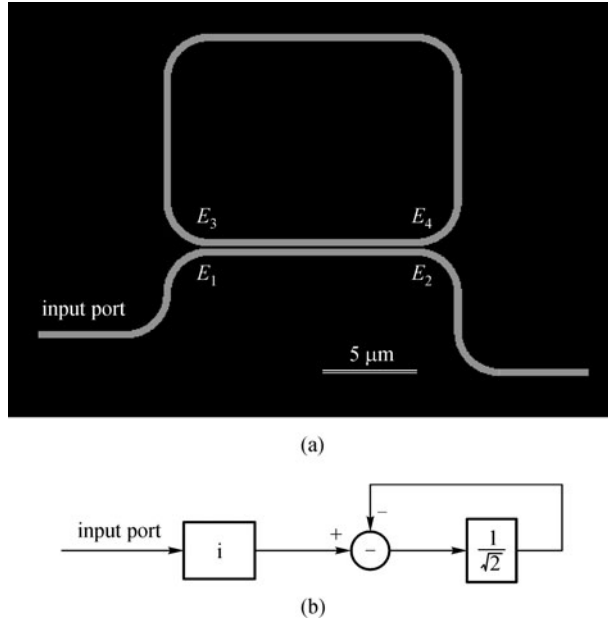


Fig. 3 (a) Loop and 3 dB directional coupler together to realize the subtractor; (b) equivalent block diagram

factor of $1/\sqrt{2}$ from the 3 dB directional coupler, and acts as an attenuator in the loop.

3 dB splitter used in our design is a bend-waveguide-type, as shown in Fig. 4(a). Considering both compactness and bend loss, the radius of the bends is supposed to be $2\ \mu\text{m}$. As demonstrated in Ref. [13], this structure features low energy loss for transverse electric (TE) mode optical signal. Equation (4) reveals the relation between E_3 and E_4 after the addition of splitter into the loop. Figures 4(b) and 4(c) show the loop with the splitter added and the corresponding block diagram, where the phase condition in Eq. (4) should be maintained. Two cascaded blocks with factors of $1/\sqrt{2}$ can be combined as a $1/2$ attenuator.

$$E_3 = \frac{1}{\sqrt{2}} e^{-j(2n+1)\pi} E_4 = -\frac{1}{\sqrt{2}} E_4. \quad (4)$$

To realize the expected function, a silicon microring resonator is used as a temporal differentiator in the structure, for its advantages of compact size, good performance and compatibility with on-chip integration [1]. The microring resonator is evanescently coupled to a single straight waveguide as shown in Fig. 5.

The transfer function of the microring resonator can be expressed as [14]:

$$T(\omega) = \frac{j(\omega - \omega_0) + \frac{1}{\tau_i} - \frac{1}{\tau_e}}{j(\omega - \omega_0) + \frac{1}{\tau_i} + \frac{1}{\tau_e}}, \quad (5)$$

where ω_0 is the central resonance frequency, τ_i represents

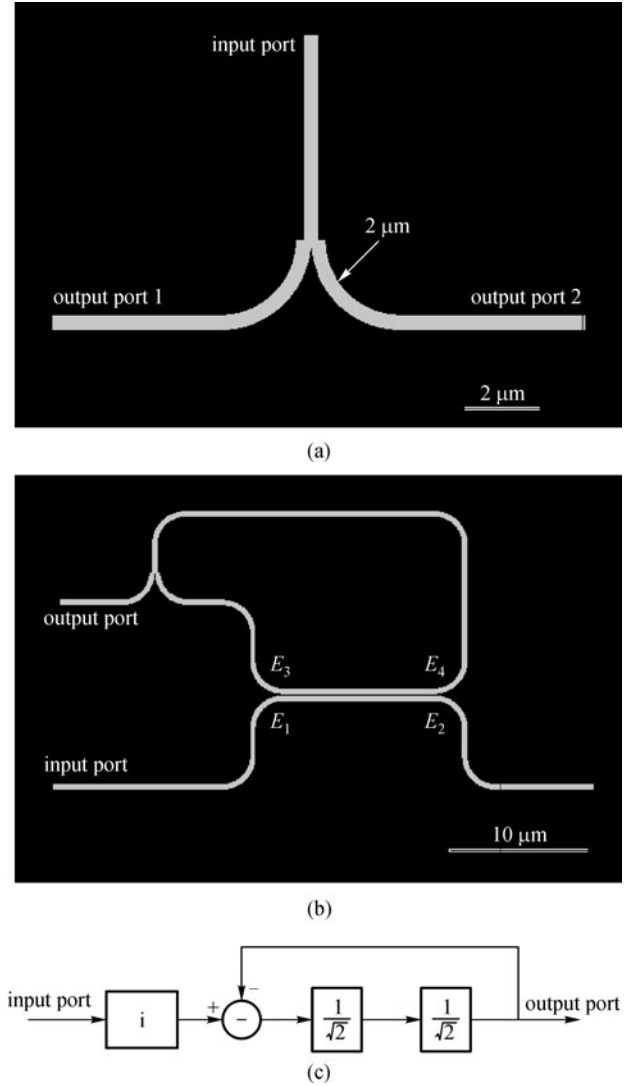


Fig. 4 (a) 3 dB bend-waveguide-type splitter; (b) loop with the splitter and an output port; (c) equivalent block diagram

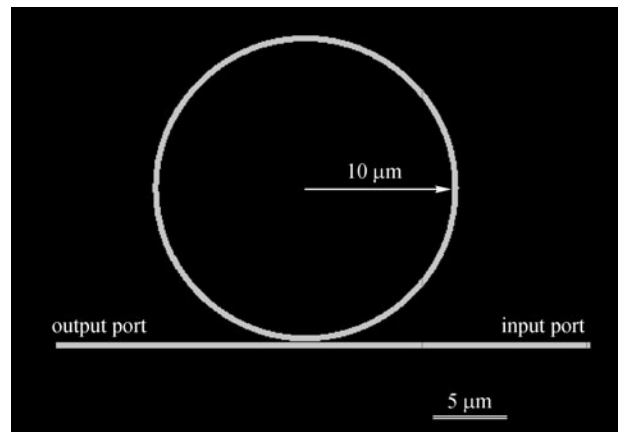


Fig. 5 Microring resonator coupled to straight waveguide

the time constant of power decay due to the intrinsic loss and τ_e is the time constant of power coupling loss to the straight waveguide from the ring. Under the condition that the microring resonator is critically coupled to the straight waveguide ($\tau_i = \tau_e$) and the frequency detuning is much less than the 3 dB bandwidth of the microring resonator, the expression can be approximated as:

$$T(\omega) = j\tau(\omega - \omega_0), \quad (6)$$

where $\frac{1}{\tau} = \frac{1}{\tau_i} + \frac{1}{\tau_e}$. As Eq. (6) reveals, the microring resonator functions as a first-order differentiator for an optical signal with the central frequency ω_0 .

To ensure that the designed structure operate correctly, two phase conditions should be satisfied at the same optical frequency: the phase shift along the microring should equal to $2k\pi$, where k is an integer, so that the frequency ω_0 is the resonance frequency of the microring resonator; and simultaneously the phase shift along the loop should be $(2n + 1)\pi$ in order to realize the function of subtractor. To satisfy these phase conditions, thermal nonlinear effect [15] of the microring resonator can be utilized to shift the resonance frequency slightly to meet two phase conditions simultaneously at the same frequency.

3 Simulations and results

Finite-difference time-domain (FDTD) method is a powerful and effective tool for simulating electromagnetic field properties of an arbitrary structure with a high index contrast. However, a quite large computer memory and a long computing time are required in a three-dimensional (3D) FDTD simulation. To reduce calculational time, two-dimensional (2D) FDTD method with the equivalent index approximation is utilized, and it has been proved to be an effective method to obtain a reasonable estimation [13].

The cross section of the silicon waveguide we used is $400 \text{ nm} \times 220 \text{ nm}$ on top of a $3 \mu\text{m}$ silica buffer layer to prevent optical mode from leaking to the substrate. This basic cross-section structure is simulated using RF module of the COMSOL Multiphysics simulation software to get the effective index of the straight waveguide, as shown in Fig. 6. Indices of Si, SiO_2 and air are assumed to be 3.478, 1.455 and 1.0, respectively. The waveguide satisfies the single mode condition at $\lambda = 1.55 \mu\text{m}$ and the mode existing is the TE mode. The simulated effective index N_{eff} is 2.1145. The top view of a silicon waveguide in 2D FDTD simulation is shown in Fig. 7. To obtain the same effective index of the waveguide in 2D FDTD simulation as in COMSOL, the equivalent index N_{eq} of Si is assumed to be 2.7533.

A loop and a microring in the structure make it impossible to simulate with the default several-femtoseconds-long pulse source, because the delay in the

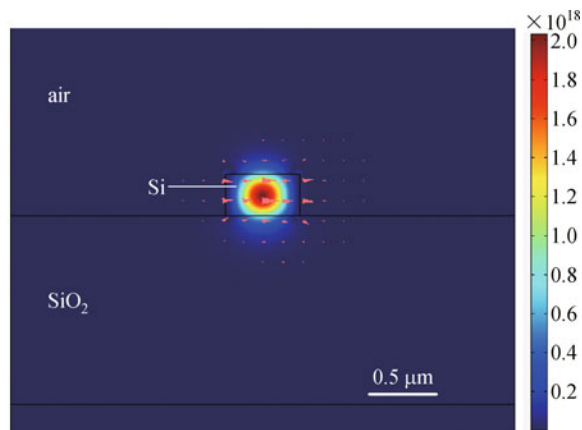


Fig. 6 Cross section of silicon waveguide based on SOI structure. Colored surface graph represents average power flow in waveguide and quivers represent electric field

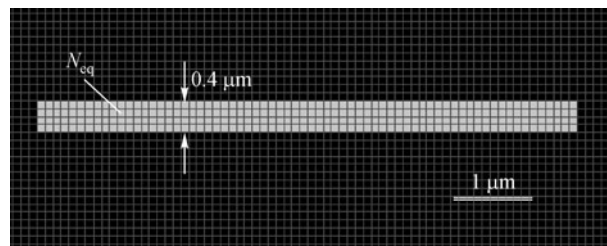


Fig. 7 Top view of silicon waveguide in 2D FDTD

microring and the loop is on the order of one picosecond. A continuous wave (CW) source, instead, is required in the simulation, which greatly increases the computing time. To further improve the efficiency of simulation, a simplified numerical simulation program coded with MATLAB based on the known linear features of microring resonator, directional coupler and 3 dB splitter is also used. In the MATLAB program, we calculate the normalized complex amplitudes of the electric field at several crucial locations of the structure with a step equal to the recirculating time of the microring. By this means, one can obtain the responses in time domain for any kind of input optical signals, including the CW signal. The validity of this coded program is verified by comparing with the simulated results of FDTD. Figure 8 provides some simulation results with two different methods.

Figure 8(c) shows that several picoseconds are needed for the loop to become stable for a step input signal.

The following simulations are based on the 2D FDTD method with the equivalent index approximation and the coded numerical simulation program. Figure 9 illustrates the whole structure of the simulated ODE computing unit. In the simplified numerical simulation, intrinsic losses of directional coupler and splitter are not considered as the value is too small to have obvious influence on the overall performance.

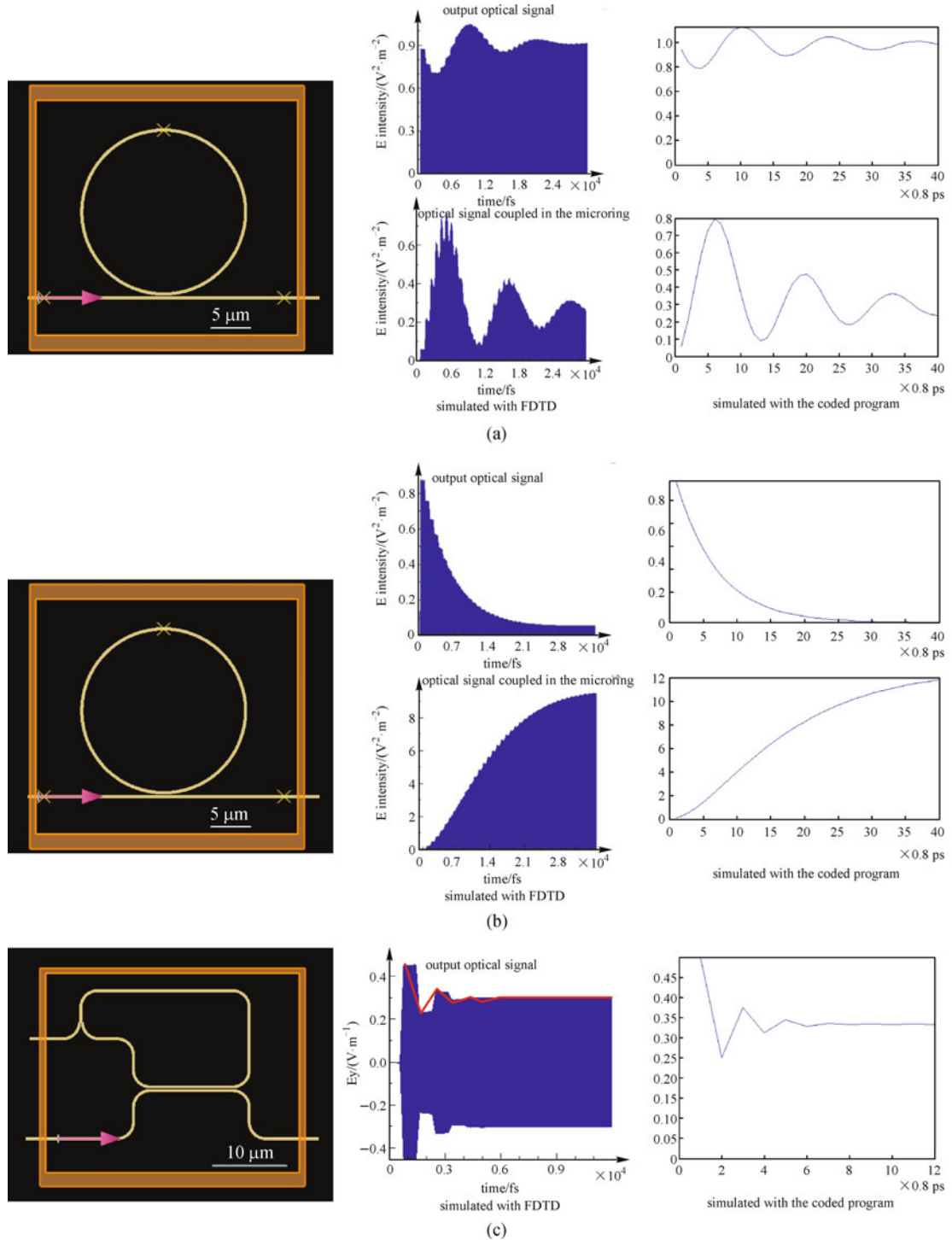


Fig. 8 Output optical intensity waveforms and optical intensity signals coupled in ring under a step input signal at optical frequency (a) $\omega \neq \omega_0$; (b) $\omega \approx \omega_0$; (c) output optical signal of loop without differentiator under a step input signal

Some simulated results and corresponding theoretical solutions of the ODE are compared in Fig. 10. The curves depict the complex amplitude of inputs and outputs. For convenience of comparison, the maximum values of input signals in Figs. 10(a)–10(c) and 10(d) are normalized to 100 and 2500, respectively. The testing waveforms include

triangle wave, pulses with the shape of parabolic curve, saw-tooth wave and its mirror image. The differences between the simulated outputs and the theoretical solutions in amplitude and shape are caused by the bandwidth limitation of the microring resonator. Since the approximated transfer function (Eq. (6)) requires that the

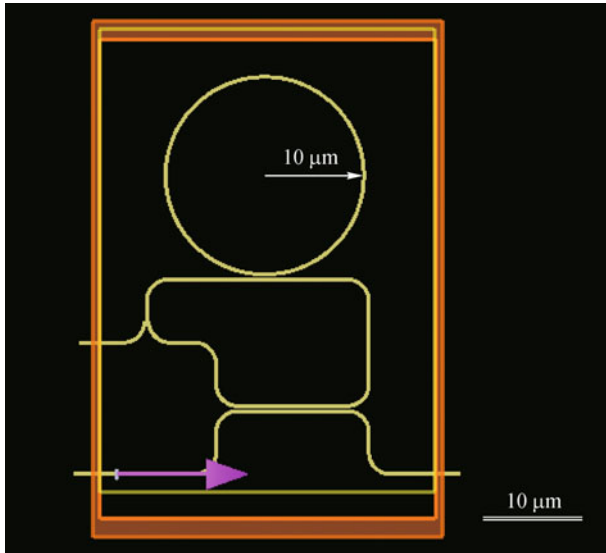
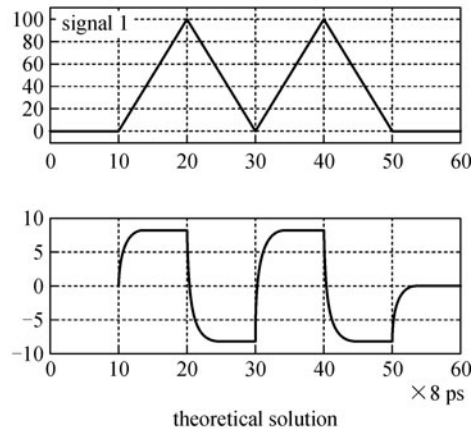
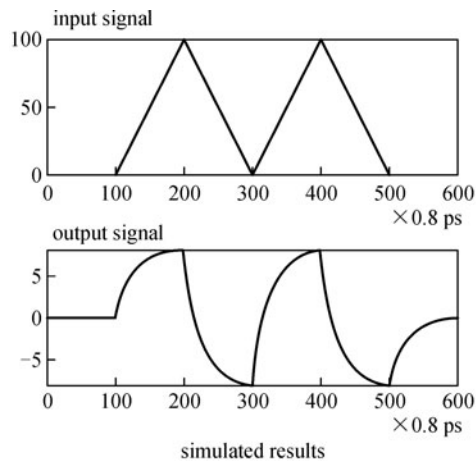
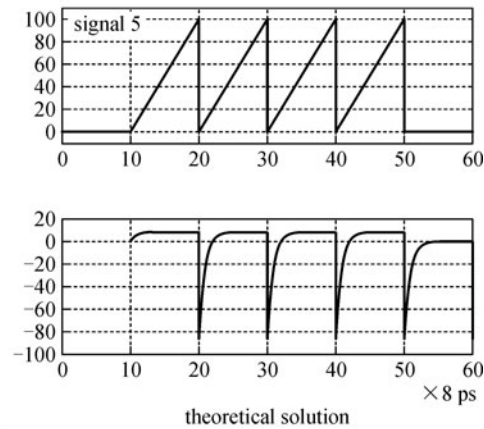
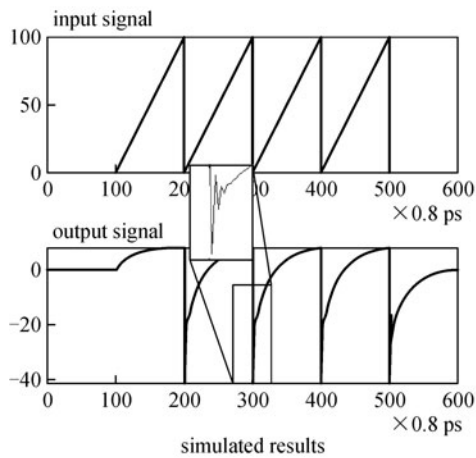


Fig. 9 Structure of simulated ODE computing unit

frequency detuning is much less than the 3 dB bandwidth of the microring resonator, the bandwidth, and thus the period of the signal, are limited. If the frequency detuning ($\omega - \omega_0$) approaches to infinite, $|T(\omega)|$ in Eq. (6) approaches to infinite as well. However, for a microring resonator, when frequency detuning becomes much larger than its 3 dB bandwidth, the transfer function only approaches to unity, because it's a passive device. As a result, for the whole structure, the transfer function of the theoretical model characterized by Fig. 1(a) approaches to 1 when $(\omega - \omega_0)$ approaches to infinite, but in the real system, it can only rise to 1/3. So the high frequency component of the output is suppressed, and causes the difference between the simulated outputs and the theoretical solutions. Stronger high-frequency components of the input signals would cause more obvious deviation of simulated outputs from theoretical ones. In Figs. 10(b) and 10(c), the sudden seesaws at the edges of output pulses are caused by the transient process of the loop, which is similar to the phenomenon shown in Fig. 8(c).



(a)



(b)

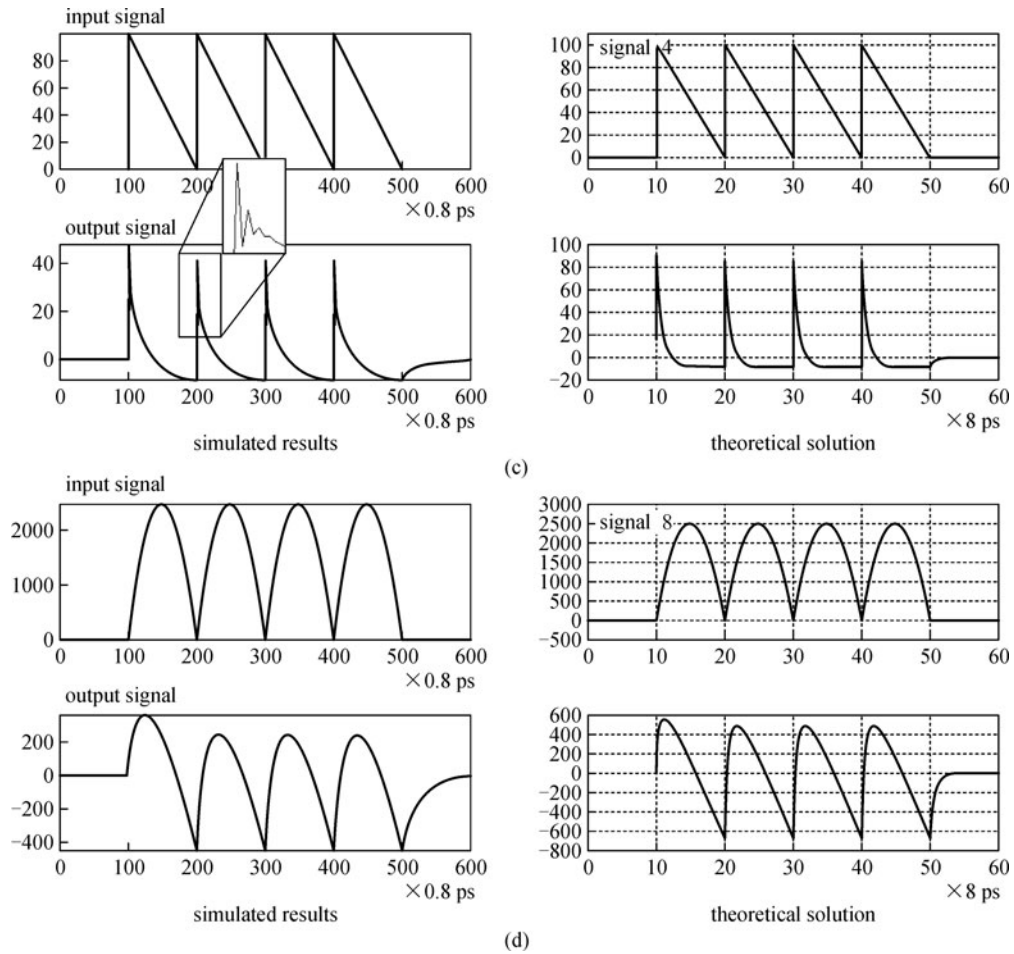


Fig. 10 Simulated output waveforms of optical ODE solver and theoretical solutions of ODE with inputs of (a) triangle wave; (b) saw-tooth wave; (c) mirror image of saw-tooth wave; (d) pulses with shape of parabolic curve

4 Conclusions

We have proposed and numerically demonstrated a compact optical temporal ODE computing unit, with its footprint within the size of only $35 \mu\text{m} \times 35 \mu\text{m}$ on an SOI platform. The device is based on a silicon microring resonator. The performance of the ODE solver is simulated with several typical signals. The comparison between simulated outputs and theoretical solutions shows the effectiveness of the compact all-optical ODE solver.

Acknowledgements This work was partly supported by the National Natural Science Foundation of China (Grant Nos. 61077052 and 61125504), Foundation of Ministry of Education of China (No. 20110073110012), and Science and Technology Commission of Shanghai Municipality (No. 11530700400).

References

- Liu F F, Wang T, Qiang L, Ye T, Zhang Z, Qiu M, Su Y. Compact optical temporal differentiator based on silicon microring resonator. *Optics Express*, 2008, 16(20): 15880–15886
- Slavik R, Park Y, Kulishov M, Morandotti R, Azaña J. Ultrafast all-optical differentiators. *Optics Express*, 2006, 14(22): 10699–10707
- Azaña J, Slavik R, Park Y, Kulishoy M. Ultrafast all-optical differentiators based on fiber gratings. In: *Proceedings of International Conference on Transparent Optical Networks*, 2007, 101–104
- Ferrera M, Park Y, Razzari L, Little B E, Chu S T, Morandotti R, Moss D J, Azaña J. On-chip CMOS-compatible all-optical integrator. *Nature Communications*, 2010, 1(29): 29
- Ngo N Q, Yu S F, Tjin S C, Kam C H. A new theoretical basis of higher-derivative optical differentiators. *Optics Communications*, 2004, 230(1–3): 115–129
- Lenz G, Eggleton B J, Madsen C K, Slusher R E. Optical delay lines based on optical filters. *IEEE Journal of Quantum Electronics*, 2001, 37(4): 525–532
- Berger N K, Levit B, Fischer B, Kulishov M, Plant D V, Azaña J. Temporal differentiation of optical signals using a phase-shifted fiber Bragg grating. *Optics Express*, 2007, 15(2): 371–381
- Xu K, Niu J, Dai Y T, Sun X, Dai J, Wu J, Lin J. All-optical analog-to-digital conversion scheme based on Sagnac loop and balanced receivers. *Applied Optics*, 2011, 50(14): 1995–2000
- Tang X G, Liao J K, Lu R G, Li H P, Zhang X X, Zhang L, Liu Y Z.

- Optical coding scheme for all-optical analog-to-digital conversion using asymmetrical Y-branch waveguide. *Optics Communications*, 2011, 284(9): 2298–2302
10. Oppenheim A V, Willsky A S, Hamid S. *Signals and Systems*. 2nd ed. Upper Saddle River, NJ: Prentice-Hall, 1996
 11. Simmons G F. *Differential Equations with Applications and Historical Notes*. 2nd ed. New York: McGraw-Hill, 1991
 12. Xu J, Zhang X L, Dong J J, Liu D M, Huang D X. All-optical differentiator based on cross-gain modulation in semiconductor optical amplifier. *Optics Letters*, 2007, 32(20): 3029–3031
 13. Sakai A, Fukazawa T, Baba T. Low loss ultra-small branches in a silicon photonic wire waveguide. *IEICE Transactions on Electronics*. E (Norwalk, Conn.), 2002, 85-C(4): 1033–1038
 14. Zhang Z Y, Dainese M, Wosinski L, Qiu M. Resonance-splitting and enhanced notch depth in SOI ring resonators with mutual mode coupling. *Optics Express*, 2008, 16(7): 4621–4630
 15. Liu F F, Li Q, Zhang Z Y, Qiu M, Su Y K. Optically tunable delay line in silicon microring resonator based on thermal nonlinear effect. *IEEE Journal on Selected Topics in Quantum Electronics*, 2008, 14(3): 706–712